Journal of Physics: Conference Series **1526** (2020) 012003 doi:10.1088/1742-6596/1526/1/012003

New Result on $K^+ \to \pi^+\nu\bar{\nu}$ from the NA62 Experiment

G Ruggiero[1]

Lancaster University, UK

E-mail: giuseppe.ruggiero@cern.ch

Abstract. The NA62 experiment at the CERN SPS is designed to measure the branching ratio of the $K^+ \to \pi^+\nu\bar{\nu}$ with a decay-in-flight technique and took data in 2016–2018. The statistics collected in 2017 allows NA62 to achieve the best up–to–date single event sensitivity for $K^+ \to \pi^+\nu\bar{\nu}$ corresponding to more than 2 Standard Model $K^+ \to \pi^+\nu\bar{\nu}$ expected events. The analysis of the 2017 data has revealed 2 candidate $K^+ \to \pi^+\nu\bar{\nu}$ events, while 1.5 background were expected. Together with the candidate found on the 2016 data, this result leads to 1.85×10^{-10} as preliminary upper limit at 90% C.L. on the branching ratio of the $K^+ \to \pi^+\nu\bar{\nu}$ decay. The 2017 data also allow NA62 to achieve the best up–to–date sensitivity on the search for the $\pi^0 \to$ *invisible* decay.

1. Introduction

The $K^+ \to \pi^+\nu\bar{\nu}$ ($\pi\nu\nu$) is a flavour changing neutral current decay proceeding through box and electroweak penguin diagrams. A quadratic GIM mechanism and the transition of the quark top into the quark down make this process extremely rare. The Standard Model (SM) predicts [1] the branching ratio (BR) to be $(8.4 \pm 1.0) \times 10^{-11}$, where the precision on the external inputs dominates the uncertainty. The theoretical accuracy, instead, is at the level of 2% [2].

[1] for the NA62 Collaboration: R. Aliberti, F. Ambrosino, R. Ammendola, B. Angelucci, A. Antonelli, G. Anzivino, R. Arcidiacono, T. Bache, M. Barbanera, J. Bernhard, A. Biagioni, L. Bician, C. Biino, A. Bizzeti, T. Blazek, B. Bloch-Devaux, V. Bonaiuto, M. Boretto, M. Bragadireanu, D. Britton, F. Brizioli, M.B. Brunetti, D. Bryman, F. Bucci, T. Capussela, J. Carmignani, A. Ceccucci, P. Cenci, V. Cerny, C. Cerri, B. Checcucci, A. Conovaloff, P. Cooper, E. Cortina Gil, M. Corvino, F. Costantini, A. Cotta Ramusino, D. Coward, G. D'Agostini, J. Dainton, P. Dalpiaz, H. Danielsson, N. De Simone, D. Di Filippo, L. Di Lella, N. Doble, B. Dobrich, F. Duval, V. Duk, J. Engelfried, T. Enik, N. Estrada-Tristan, V. Falaleev, R. Fantechi, V. Fascianelli, L. Federici, S. Fedotov, A. Filippi, M. Fiorini, J. Fry, J. Fu, A. Fucci, L. Fulton, E. Gamberini, L. Gatignon, G. Georgiev, S. Ghinescu, A. Gianoli, M. Giorgi, S. Giudici, F. Gonnella, E. Goudzovski, C. Graham, R. Guida, E. Gushchin, F. Hahn, H. Heath, E.B. Holzer, T. Husek, O. Hutanu, D. Hutchcroft, L. Iacobuzio, E. Iacopini, E. Imbergamo, B. Jenninger, J. Jerhot, R.W. Jones, K. Kampf, V. Kekelidze, S. Kholodenko, G. Khoriauli, A. Khotyantsev, A. Kleimenova, A. Korotkova, M. Koval, V. Kozhuharov, Z. Kucerova, Y. Kudenko, J. Kunze, V. Kurochka, V. Kurshetsov, G. Lanfranchi, G. Lamanna, E. Lari, G. Latino, P. Laycock, C. Lazzeroni, M. Lenti, G. Lehmann Miotto, E. Leonardi, P. Lichard, L. Litov, R. Lollini, D. Lomidze, A. Lonardo, P. Lubrano, M. Lupi, N. Lurkin, D. Madigozhin, I. Mannelli, G. Mannocchi, A. Mapelli, F. Marchetto, R. Marchevski, S. Martellotti, P. Massarotti, K. Massri, E. Maurice, M. Medvedeva, A. Mefodev, E. Menichetti, E. Migliore, E. Minucci, M. Mirra, M. Misheva, N. Molokanova, M. Moulson, S. Movchan, M. Napolitano, I. Neri, F. Newson, A. Norton, M. Noy, T. Numao, V. Obraztsov, A. Ostankov, S. Padolski, R. Page, V. Palladino, A. Parenti, C. Parkinson, E. Pedreschi, M. Pepe, M. Perrin-Terrin, L. Peruzzo, P. Petrov, Y. Petrov, F. Petrucci, R. Piandani, M. Piccini, J. Pinzino, I. Polenkevich, L. Pontisso, Yu. Potrebenikov, D. Protopopescu, M. Raggi, A. Romano, P. Rubin, G. Ruggiero, V. Ryjov, A. Salamon, C. Santoni, G. Saracino, F. Sargeni, S. Schuchmann, V. Semenov, A. Sergi, A. Shaikhiev, S. Shkarovskiy, D. Soldi, V. Sugonyaev, M. Sozzi, T. Spadaro, F. Spinella, A. Sturgess, J. Swallow, S. Trilov, P. Valente, B. Velghe, S. Venditti, P. Vicini, R. Volpe, M. Vormstein, H. Wahl, R. Wanke, B. Wrona, O. Yushchenko, M. Zamkovsky, A. Zinchenko.

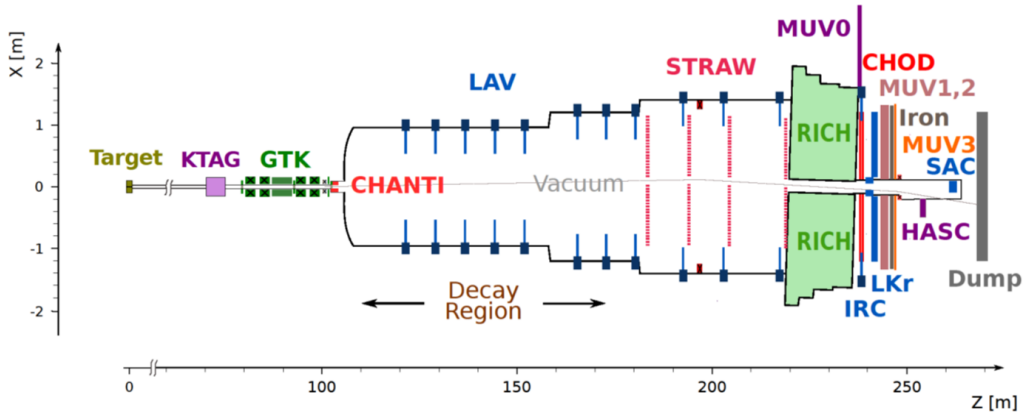

Figure 1. Schematic layout of the NA62 experiment in the xz plane.

The $K^+ \to \pi^+\nu\bar{\nu}$ decay is extremely sensitive to physics beyond the SM, probing the highest mass scales among the rare meson decays. The largest deviations from SM are expected in models with new sources of flavour violation [3] [4]. Depending on new physics models, correlation patterns between possible deviations from the SM prediction of $K^+ \to \pi^+\nu\bar{\nu}$ and $K_L \to \pi^0\nu\bar{\nu}$ decay modes can be expected [5]. Present experimental constraints limit the range of variation within supersymmetric models [6] [7] [8]. The $K^+ \to \pi^+\nu\bar{\nu}$ decay can also be sensitive to effects of lepton flavour non–universality [9] and can constrain leptoquark models [10].

The experiments E787 and E949 at BNL [11] [12] studied the $K^+ \to \pi^+\nu\bar{\nu}$ decay using a kaon decay–at–rest technique, reaching a single event sensitivity of about 0.8×10^{-10}. The measured BR is $(17.3^{+11.5}_{-10.5}) \times 10^{-11}$. The NA62 experiment at CERN aims to precisely measure the BR of the $K^+ \to \pi^+\nu\bar{\nu}$ decay with a novel kaon decay–in–flight technique. The first result of NA62 based on the analysis of the data collected in 2016 demonstrated the validity of this technique [13]. The result presented here is based on the analysis of the data collected in 2017.

2. The NA62 Experiment at CERN

The NA62 experiment is a fixed target experiment located at CERN. Fig. 1 shows a schematic view of the apparatus. The detailed description of the apparatus can be found in [14]. Primary SPS protons strike a target from which a secondary charged hadron beam of 75 GeV/c and 1% momentum bite is selected and transported downstream. About 6% of beam particles are K^+. A Cherenkov counter (KTAG) and three stations of Si pixel detectors (GTK) identifies the K^+ and traces the beam particles, respectively. A decay tank, holding a 10^{-6} mbar vacuum, forms the region downstream to the beam line. A collimator (final collimator) separates this region from the beam line, blocking the non–muonic beam–related activity. The last station of the GTK is placed in the decay tank, just downstream to the final collimator. A guard ring detector (CHANTI) vetoes beam inelastic interactions occurring in this GTK station. Annular lead-glass calorimeters (LAV) surround the region downstream of the beam line for high angle photon detection. Four stations of straw chambers (STRAW) in vacuum trace downstream charged particles measuring their momentum. A RICH counter time-stamps and identifies charged particles. Plastic scintillators (CHOD) are used for triggering and timing. An electromagnetic calorimeter of liquid krypton (LKr) and small angle calorimeters (IRC and SAC) ensure photon detection in the forward region. Hadron calorimeters (MUV1,2) and a plastic scintillator detector (MUV3) are used to identify muons. Information from CHOD, RICH, MUV3 and LKr are built up online to issue level zero trigger conditions [15]. Software-based variables from KTAG,

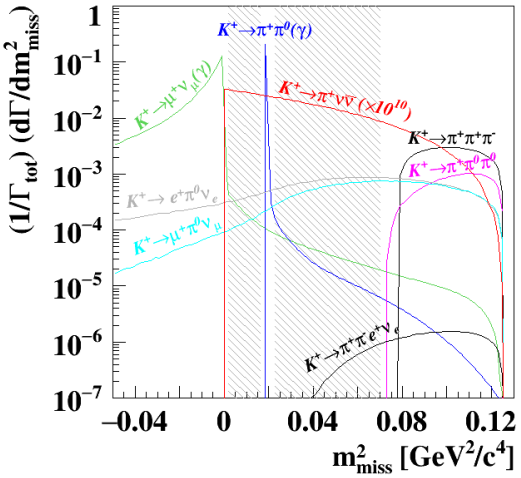

Figure 2. m^2_{miss} of K^+ decays relevant to the $K^+ \to \pi^+\nu\bar{\nu}$ measurement. The m^2_{miss} is computed under the hypothesis that the charged particle in the final state is a π^+. Signal (red) is multiplied by 10^{10} for visibility. The dashes area denote the regions where to search for signal.

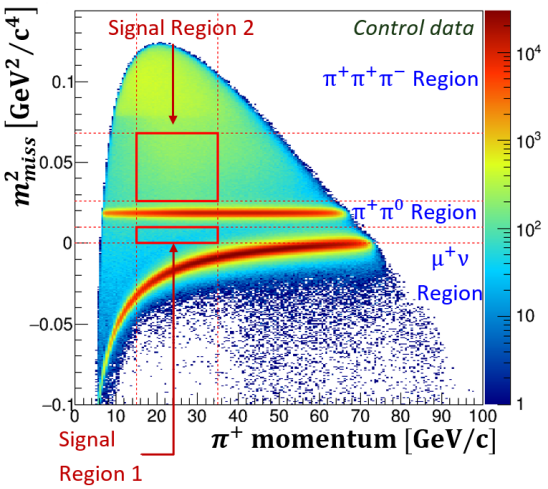

Figure 3. m^2_{miss} versus π^+ momentum of selected K^+ decays on minimum bias data. The signal regions 1 and 2 and the three background regions are also indicated.

CHOD, LAV and STRAW provide higher level trigger requirements. Data for $\pi\nu\nu$ are taken concurrently with downscaled samples of data for rare kaon decays studies and minimum bias.

NA62 ran in 2016, 2017 and 2018. In 2017 the SPS has delivered about 1.9×10^{12} protons per pulse, corresponding to about 450 MHz particle rate in GTK.

3. Principle of the Measurement

The signature of a $K^+ \to \pi^+\nu\bar{\nu}$ decay is one K^+ in the initial state and one π^+ with missing energy in the final state. The main kinematic variable is $m^2_{miss} \equiv (P_K - P_\pi)^2$, where P_K and P_π are the 4-momenta of the K^+ and π^+, respectively. The m^2_{miss} of the signal is broadly distributed, as shown in Fig. 2. Search for signal occurs in two regions of the m^2_{miss} spectrum across the $K^+ \to \pi^+\pi^0$ peak. Possible backgrounds are: $K^+ \to \pi^+\pi^0$, $K^+ \to \mu^+\nu$ and $K^+ \to \pi^+\pi^+\pi^-$ entering signal regions through non gaussian resolution and radiative tails of the m^2_{miss}, if any; $K^+ \to l^+\pi^0\nu_l$ decays and more rare processes like $K^+ \to \pi^+\pi^-e^+\nu$ broadly distributed across the signal regions; events mimicking $K^+ \to \pi^+\nu\bar{\nu}$ originating along the beam line via inelastic interactions of beam particles with the material; K^+s that decay before entering the fiducial volume downstream to the last station of the GTK (GTK3). Each source of background requires different rejection procedures, depending on the kinematics and on the type of charged particle in the final state. The estimation of the expected background remaining after selection is done separately for each process. A blind analysis procedure has been adopted, with signal and control regions kept masked until completion of the selection criteria and the evaluation of the signal and background.

4. Selection

A STRAW track associated to signals in RICH, LKr and CHOD defines a π^+. A signal in KTAG associated to a GTK track defines a K^+. The K^+ is coupled to the π^+ by matching in time and space the corresponding tracks. Selection criteria applied to the reconstructed decay

vertex define the fiducial decay region downstream of the last GTK station. In addition events are rejected if the π^+ track originates from the beam aperture of the final collimator.

Fig. 3 shows the distribution of the selected events in the (m^2_{miss}, p_{π^+}) plane. Here p_{π^+} is the π^+ momentum. The m^2_{miss} is computed using the K^+ and π^+ momenta measured in GTK and STRAW assuming the K^+ and π^+ masses, respectively. This plane defines two signal regions, termed Signal Region 1 and 2, and three background regions mostly populated by $K^+ \to \pi^+\pi^0$, $K^+ \to \mu^+\nu$ and $K^+ \to \pi^+\pi^+\pi^-$ decays. The $\pi\nu\nu$ analysis is restricted to $(15, 35)\,\mathrm{GeV/c}$ π^+ momentum, leaving at least 40 GeV of extra energy to veto background events.

The selection proceeds with the π^+ identification using the calorimeters and the RICH. Eventually events with muons are suppressed by 8 orders of magnitude.

Events with photons are rejected by exploiting the time coincidence between the π^+ and possible signals in LAV, LKr, IRC or SAC. Selection criteria based on CHOD's and STRAW's activity are employed against photons interacting with the material upstream of the LKr. The π^0 detection inefficiency is about 1.4×10^{-8}, measured on data. The above criteria are also effective against decays like $K^+ \to \pi^+\pi^+\pi^-$ and $K^+ \to \pi^+\pi^- e^+\nu$. Finally events are excluded in presence of CHANTI signals in time with the π^+ or extra hits in at least 2 GTK stations.

The $K^+ \to \pi^+\nu\bar{\nu}$ candidates are those events in regions 1 and 2 that pass the selection criteria described above.

5. Single Event Sensitivity

The number of expected SM $K^+ \to \pi^+\nu\bar{\nu}$ events, $N_{\pi\nu\nu}$, is estimated as:

$$N_{\pi\nu\nu} = N_{\pi\pi}\epsilon_{trig}\epsilon_{RV}\frac{A_{\pi\nu\nu}}{A_{\pi\pi}}\frac{BR(\pi\nu\nu)}{BR(\pi\pi)}. \quad (1)$$

Here $N_{\pi\pi}$ is the number of $K^+ \to \pi^+\pi^0$ decays selected on minimum bias data. The same offline $\pi\nu\nu$ selection criteria are used to this purpose, but the photon rejection cuts and requiring the m^2_{miss} in the $K^+ \to \pi^+\pi^0$ region. The symbols ϵ_{trig} and ϵ_{RV} denote the $\pi\nu\nu$ trigger and the random veto efficiencies, both measured on data. In particular ϵ_{RV} is defined as one minus the probability for a signal event to be randomly rejected by the photon veto conditions; it is about 64% on average and depends on the beam intensity. The symbols $A_{\pi\nu\nu}$ and $A_{\pi\pi}$ denote the geometrical and selection acceptances for signal and $K^+ \to \pi^+\pi^0$ decays, estimated from Monte Carlo simulations. Finally $BR(\pi\nu\nu)$ and $BR(\pi\pi)$ are the predicted by the SM and measured branching ratios of the $K^+ \to \pi^+\nu\bar{\nu}$ and the $K^+ \to \pi^+\pi^0$ decays [16], respectively. The number $N_{\pi\nu\nu}$ is evaluated in four bins of π^+ momentum. The efficiencies ϵ_{trig} and ϵ_{RV} are combined taking into account their dependence on the instantaneous beam intensity. The activity in the time sidebands of the GTK allows for the estimation of the instantaneous beam intensity event–by–event.

By definition, the single event sensitivity (SES) is equal to $BR(\pi\nu\nu)/N_{\pi\nu\nu}$.

The measured SES is $(0.389 \pm 0.021) \times 10^{-10}$ corresponding to $N_{\pi\nu\nu} = 2.16 \pm 0.12 \pm 0.26_{ext}$. The uncertainty of SES is systematical and mostly stems from the evaluation of ϵ_{trig} and $A_{\pi\nu\nu}$. The external uncertainty of $N_{\pi\nu\nu}$ comes from the theoretical error on $BR(\pi\nu\nu)$. The achieved sensitivity corresponds to about 2×10^{12} K^+ decays analyzed.

6. Background Evaluation

Table 1 summarizes the expected backgrounds in regions 1 and 2 after the $\pi\nu\nu$ selection.

A class of backgrounds comes from K^+ decaying in the fiducial volume. The estimation of the $K^+ \to \pi^+\pi^0$ and $K^+ \to \mu^+\nu$ background relies on the assumption that π^0 and μ^+ rejection are

Table 1. Expected signal and background events. $K^+ \to \pi^+\pi^0(\gamma)$ IB and $K^+ \to \mu^+\nu_\mu(\gamma)$ IB include also the contribution from the inner Bremsstrahlung radiation.

Process	Expected events
$K^+ \to \pi^+\nu\bar{\nu}$	$2.16 \pm 0.12_{syst} \pm 0.26_{ext}$
$K^+ \to \pi^+\pi^0(\gamma)$ IB	$0.29 \pm 0.03_{stat} \pm 0.03_{syst}$
$K^+ \to \mu^+\nu_\mu(\gamma)$ IB	$0.11 \pm 0.02_{stat} \pm 0.03_{syst}$
$K^+ \to \mu^+\nu_\mu\,(\mu^+ \to e^+ decay)$	$0.04 \pm 0.02_{syst}$
$K^+ \to \pi^+\pi^-e^+\nu_e$	$0.12 \pm 0.05_{stat} \pm 0.03_{syst}$
$K^+ \to \pi^+\pi^+\pi^-$	$0.02 \pm 0.02_{syst}$
$K^+ \to \pi^+\gamma\gamma$	$0.005 \pm 0.005_{syst}$
$K^+ \to l^+\pi^0\nu_l\,(l = e^+, \mu^+)$	negligible
Upstream background	$0.9 \pm 0.2_{stat} \pm 0.2_{syst}$
Total background	$1.5 \pm 0.2_{stat} \pm 0.2_{syst}$

independent from the m^2_{miss} cuts defining the signal regions. Kinematically unbiased samples of $K^+ \to \pi^+\pi^0$ and $K^+ \to \mu^+\nu$ events selected on minimum bias data provide a measurement of the probability for these decays to enter the signal regions as a consequence of a mis–reconstructed kinematics. The expected background stems from this probability and the number of events surviving the $\pi\nu\nu$ selection in the corresponding m^2_{miss} background regions. Corrections are applied to account for correlations between kinematics and π^0 and μ^+ rejections using both simulations and data. The agreement between expected and observed background events in suitable control regions of the m^2_{miss} validates the estimation of these backgrounds. A similar procedure is adopted to assess the $K^+ \to \pi^+\pi^+\pi^-$ background. The estimation of the other backgrounds from K^+ decays relies on Monte Carlo simulations normalized to $K^+ \to \pi^+\pi^0$ decays, as for the signal. Samples of background–enriched data are used to validate the simulation down to the $\pi\nu\nu$ single event sensitivity.

Upstream background events are π^+s originated by decays or interactions of K^+s occurring upstream of the final collimator. In these cases a lone π^+ can enter the region downstream through the beam aperture of the final collimator, with the collimator itself preventing the detection of the extra energy produced concurrently with the π^+. The π^+ mimics a signal event if accidentally matched to a random beam particle. In addition the direction of the π^+ must be mis–reconstructed to create a fake decay vertex in the fiducial volume and to trace back the π^+ outside the beam aperture of the final collimator. The estimation of the upstream background exploits the probability of an accidental matching of a π^+ to a random beam track and the total number of events surviving the $\pi\nu\nu$ selection, with the criteria of $K^+ - \pi^+$ association inverted.

The analysis described above is repeated in the $(35, 40)\,\mathrm{GeV/c}$ π^+ momentum range. In this case about 0.62 background and 0.13 signal events are expected in the m^2_{miss} ranges equivalent to regions 1 and 2, while 1 event is observed. This result eventually validates the background estimation procedure.

7. Result

Fig. 4 shows the m^2_{miss} versus p_{π^+} distribution of the events passing the $\pi\nu\nu$ selection. Two events are observed in the signal regions, in agreement with the 2.16 signal and 1.5 background events expected. The observed events in the $(15, 35)\,\mathrm{GeV/c}$ π^+ momentum region compared with the expected backgrounds is depicted in Fig. 5. The combination of the 2016 and 2017 data leads to an overall $SES = (0.346 \pm 0.017) \times 10^{-10}$, with 3 signal candidates observed and

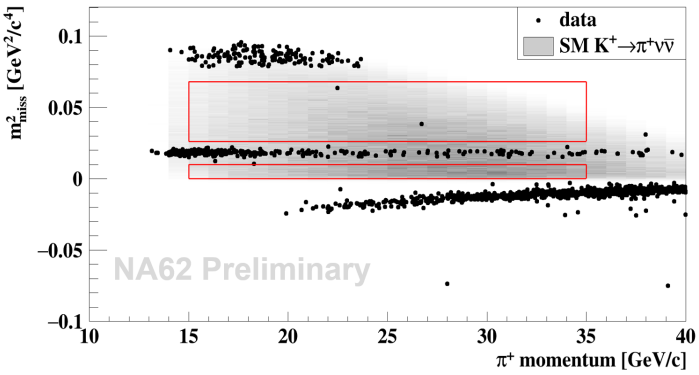

Figure 4. m^2_{miss} versus π^+ momentum of the events passing the $\pi\nu\nu$ selection. The red boxes denote the signal regions 1 and 2. The shadowed grey area is the distribution of simulated $K^+ \to \pi^+\nu\bar{\nu}$ events.

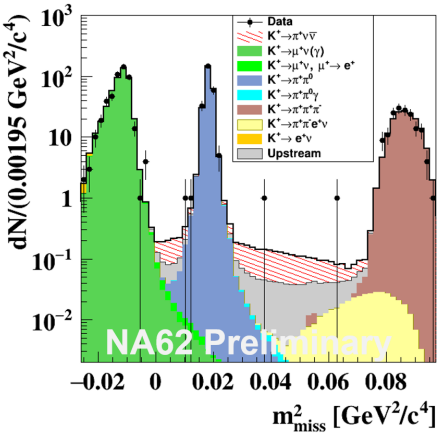

Figure 5. $m^2_{miss}$the events in the $(15, 35)$ GeV/c π^+ momentum passing the $\pi\nu\nu$ selection, compared to the expected signal and background. Both data and Monte Carlo samples are used to derive the shape of the m^2_{miss} for the various backgrounds.

1.65 ± 0.31 background events expected. Using the CLs method [17], a simple events counting approach gives a preliminary observed upper limit $BR(K^+ \to \pi^+\nu\bar{\nu}) < 1.85 \times 10^{-10}$ at 90% C.L. The corresponding 90% C.L. expected upper limit is 1.32×10^{-10}.

8. Search for $\pi^0 \to invisible$

The achieved level of π^0 rejection allows for a significant improvement in the search for the decay $\pi^0 \to invisible$ with respect to the existing upper limit [18]. The analysis makes use of the same $\pi\nu\nu$ selection applied to about one third of the 2017 $\pi\nu\nu$ data. An a–priori study of the π^0 rejection is carried on before counting the residual events in the $K^+ \to \pi^+\pi^0$ m^2_{miss} region. This study proceeds through an evaluation of the single–γ detection efficiency by exploiting a tag–and–probe method on a sample of $K^+ \to \pi^+\pi^0$ decays selected on minimum bias data. The expected π^0 efficiency stems from the single–γ detection efficiency convoluted with simulated $K^+ \to \pi^+\pi^0$ decays. The π^0 efficiency depends on the π^+ momentum. The optimal momentum region is $(25-40)$ GeV/c, corresponding to a π^0 detection inefficiency of $(2.8^{+5.0}_{-2.1}) \times 10^{-9}$. The π^+ momentum side–bands where the inefficiency is above 10^{-7} are used for validation, as the current upper limit here excludes the $\pi^0 \to invisible$. The result on the π^0 efficiency translates into 10^{+22}_{-8} expected $K^+ \to \pi^+\pi^0$ in the corresponding m^2_{miss} region. Twelves events are observed, leading to an upper limit $BR(\pi^0 \to invisible) < 4.4 \times 10^{-9}$ at 90% C.L.

9. Conclusions

The NA62 experiment analyzed the data collected in 2017 achieving the best up–to–date single event sensitivity to the $K^+ \to \pi^+\nu\bar{\nu}$ decay. In total 3 signal–candidate events have been observed in the 2016 and 2017 data, leading to a preliminary upper limit $BR(K^+ \to \pi^+\nu\bar{\nu}) < 1.85 \times 10^{-10}$ at 90% C.L. This result translates into a 90% C.L Grossman–Nir limit [19] on the SM $K_L \to \pi^0\nu\bar{\nu}$ branching ratio equal to 8.14×10^{-10}. The 2017 data also allows NA62 to achieve the highest sensitivity to the search for the $\pi^0 \to invisible$ decay.

References

[1] Buras A J, Buttazzo D, Girrbach–Noe J and Knegjens R 2015 *JHEP* **1511** 033
[2] Brod J, Gorbahn M and Stamou E 2011 *Phys. Rev.* D **83** 034030
[3] Blanke M, Buras A J and Recksiegel S 2016 *Eur. Phys. J.* C **76** no.4 182
[4] Blanke M, Buras A J, Duling B, Gemmler K and Gori S 2009 *JHEP* **0903** 108
[5] Buras A J, Buttazzo D and Knegjens R 2015 *JHEP* **1511** 166
[6] Isidori G, Mescia F, Paradisi P, Smith C and Trine S 2006 *JHEP* **0608** 064
[7] Blazek T and Matak P 2010 *Nucl. Phys. Proc. Suppl.* **198** 216
[8] Tanimoto M and Yamamoto K 2016 *PTEP* **2016** no.12 123B02
[9] Bordone M, Buttazzo D, Isidori G and Monnard J 2017 *Eur. Phys. J.* C **77** no.9 618
[10] Bobeth C and Buras A J 2018 *JHEP* **1802** 101
[11] Artamonov A V *et al* 2008 *Phys. Rev. Lett.* **101** 191802
[12] Artamonov A V *et al* 2008 *Phys. Rev.* D **79** 092004
[13] Cortina Gil E *et al* 2019 *Phys. Lett.* B **791** 156–66.
[14] Cortina Gil E *et al* 2017 *J. Instrum.* **12** P05025
[15] Ammendola R *et al* 2019 *Nucl. Instrum. Meth.* A **929** 001–022
[16] Tanabashi M *et al.* [Particle Data Group] 2018 *Phys. Rev.* D **98** no. 3 030001
[17] Read A L 2002 *J. Phys.* G **28** 2693
[18] Artamonov A V*et al* 2005 *Phys. Rev.* D **72** 091102
[19] Grossman Y and Nir Y 1997 *Phys. Lett.* B **398** 163